

Single Forces and Double-Couples: A Theoretical Review of Their Relative Efficiency for the Excitation of Seismic and Tsunami Waves

Emile A. Okal

Department of Geological Sciences, Northwestern University,
Evanston, Illinois 60208, U.S.A.

We compare the theoretical excitation of surface waves and tsunamis by sources represented by single forces and double-couples. We first show that an average single force, whose orientation and exact depth are unknown, should excite any seismic wave proportionally to wavelength, relative to a similarly average double-couple, having the same source time function. Because of the condition of zero impulse on the whole planet, the spectrum of a single force source has an additional ω^2 factor at low frequencies. As a result, a general deficiency in long period energy is expected. However, we show on a number of examples that it can be observed only at the extreme low-frequency end of the spectrum of mantle waves, and probably would escape routine seismological observation.

We explore the possibility of identifying single force sources on the basis of single-station inversions of Love and Rayleigh waves, through the systematic inversion of synthetic spectra. Inversion of double-couple spectra for single forces (and vice versa) have variance reductions on the order of 70%, which may be too performant to allow discrimination under operational conditions, including noise and inaccurate epicentral distances. An important case is that of the pure dip-slip double-couple geometry on a purely vertical fault, which can be recognized from a single horizontal force, provided both Rayleigh and Love waves are used over a sufficiently broad range of frequencies. Previous controversy, notably in the case of the 1975 Kalapana, Hawaii earthquake, may reflect the use of band-pass filtered Love waves.

In the case of tsunami excitation, and because of the ω^2 term brought about by the condition of zero-impulse, single forces are significantly deficient tsunami generators, by as much as 1.5 orders of magnitudes, relative to a double-couple exciting comparable mantle waves. The enhanced tsunamis occasionally excited by events successfully modeled as single forces are due to the mechanical interaction of the source, whatever its nature, with softer layers in the vicinity of the surface.

1. Introduction

Over the past few years, considerable attention has been paid to the possibility of modeling certain seismic sources, specifically those involving large slumps or landslides, as single forces, rather than double-couples. These studies were initially motivated by

Received September 27, 1990; Accepted January 28, 1991

the Mount St. Helens Eruption of 18 May 1980, for which Kanamori and Given (1982 a) and later Kanamori *et al.* (1984) interpreted the long period surface waves as generated by the landslide, which they modeled as an essentially horizontal force, while the higher-frequency seismic energy could be described by a smaller vertical single force. Later, Eissler and Kanamori (1987) similarly modeled the 1975 Kalapana, Hawaii earthquake as a single force, and Hasegawa and Kanamori (1987) the 1929 Grand Banks event. Recently, Kawakatsu (1989) has extended to the case of single forces the inversion for dynamic source components introduced for double-couples as the centroid moment tensor inversion by Dziewonski *et al.* (1981), Kanamori and Given (1981, 1982b) and Romanowicz and Guillemant (1984).

In the case of well-documented landslides such as those at Mount St. Helens, or at Mantaro, Peru on 24 April 1974 (Kawakatsu, 1989), there can be little controversy as to the inadequacy of a standard double-couple seismic source. In other cases, however, the modeling of seismic events by single forces remains controversial. In particular, for the Kalapana earthquake, Harvey and Wyss (1986) and Wyss and Kovach (1988) have argued for a complex series of double-couples, rather than for the single force proposed by Eissler and Kanamori (1987, 1988), and Kawakatsu (1989) has shown that the quality of the single force inversion is actually less than when the data are inverted for a double-couple.

In addition, several events successfully (or tentatively) modeled as non double-couple sources qualify as "tsunami earthquakes," as defined by Kanamori (1972), i.e., they generated larger tsunamis than expected from their conventional magnitudes (e.g., M_s). Examples would include the 1929 Grand Banks and 1975 Kalapana earthquakes, as well as the underwater event near Tori-shima Island on 13 June 1984, modeled by Barker and Kanamori (1986) and Kanamori *et al.* (1986) as a Compensated Linear Vector Dipole (CLVD). This has led to the speculation that some of the larger anomalously tsunamigenic earthquakes could actually involve submarine landslides; in particular Kanamori (1985) has suggested such a mechanism for the great Aleutian event of 01 April 1946. On the other hand, Pelayo and Wiens (1990) have shown, through a careful analysis of its low-frequency mantle waves, that the tsunami earthquake of 20 November 1960 in Peru could be modeled by a genuine, albeit slow, double-couple.

The purpose of this paper is twofold: First, we review, from a theoretical standpoint, the relative efficiency of the two kinds of sources for the excitation of various seismic waves, and seek to identify crucial parameters which could provide immediate identification of a single force source at teleseismic distances, if possible in the context of the operation of an isolated, single station observatory. Second, we investigate the relative efficiency of single forces and double couples for tsunami generation.

Our major conclusions are (i) The deficiency in surface wave excitation expected at longer periods from the behavior of the source time function of a single force is tangible only at the lowest mantle frequencies (300 s and above); (ii) Inversions of mantle wave spectra (especially single-station ones) must be carried out over a broad range of frequencies, for both Rayleigh and Love waves, if they are to discriminate between single forces and double-couples; and (iii) Single forces are actually deficient tsunami generators; the large tsunamis generated by events modeled by single forces are not due

to the nature of the source, but rather to its location inside, or in the immediate vicinity of, a weak mechanical structure such as a sedimentary layer.

2. Excitation from Step-Function Sources

In this section, we compare the theoretical excitation of seismic waves in an elastic Earth by double-couples and single forces, assuming in both cases that their time behavior is that of a step function $H(t)$. While this assumption is correct (at least in the low-frequency limit) for double couples, it is clearly inappropriate for single forces, which must satisfy a condition of zero impulse (Kawakatsu, 1989). However, these results will be useful to the discussion of sources with more realistic time functions, which will be considered in the next section.

2.1 Rayleigh waves

As discussed by Kanamori and Stewart (1976), whose notation we adopt in the present paper, the source contribution to the spectral amplitude of a Rayleigh wave generated by a double-couple of moment M_0 is given by:

$$M_0 \cdot E^{\text{DC}} = M_0 \left[\frac{1}{U} |s_R K_0 l^{-1/2} - i q_R K_1 l^{1/2} - p_R K_2 l^{3/2}| \right]. \quad (1)$$

The coefficients K_i are characteristic of depth and frequency; s_R , q_R , p_R are trigonometric functions depending on the geometry of the double-couple and on the azimuth to the particular station considered, and U is the wave's group velocity. We also neglect a constant factor $a\sqrt{\pi/2}$, where a is the Earth's radius.

Similarly, the excitation of the same wave by a force F_0 with a step-function time history can be written:

$$F_0 \cdot E^{\text{SF}} = F_0 \left[\frac{1}{U} |s_F K_0^{\text{SF}} l^{-1/2} + i q_F K_1^{\text{SF}} l^{1/2}| \right], \quad (2)$$

where the new single-force excitation coefficients are related to the double-couple ones through

$$K_0^{\text{SF}} = -\frac{y_1(r_s)}{y_3(r_s)} r_s K_2 \quad (3a)$$

and

$$K_1^{\text{SF}} = -r_s K_2 \quad (3b)$$

r_s being the distance of the point source to the center of the Earth. The trigonometric coefficients become $s_F = \cos \psi$ and $q_F = \sin \psi \cos \phi$, where ψ is the colatitude of the direction of the force F_0 with respect to the local vertical, and ϕ the longitude (measured clockwise) of the azimuth of the station with respect to that of the horizontal component of F_0 (Eissler and Kanamori, 1987).

In order to discuss the general behavior of the two kinds of sources with frequency, we adopt in this section Okal and Talandier's (1989) approach, which consists of

envisioning an average focal mechanism and depth, in the general philosophy of the concept of magnitude. These authors justified

$$L^{\text{DC}} = -C_s^{\text{DC}} = \log_{10} \langle E^{\text{DC}} \rangle = -1.6163\theta^3 + 0.83322\theta^2 - 0.42861\theta - 3.7411 \quad (4)$$

(with $\theta = \log_{10} T - 1.8209$) as the best-fitting cubic spline through the logarithm of the average value of E^{DC} in (1). In other words, (4) provides an estimate of the excitability of Rayleigh waves of period T by a double-couple of arbitrary orientation and depth, the latter being constrained to shallow values ($h \leq 75$ km). On the basis of theoretical estimates, and of an extensive dataset, Okal and Talandier (1989) have shown that the error introduced by using (4) instead of the exact excitation (1) is usually less than 0.2 unit of magnitude. Note that the logarithmic average excitation, L^{DC} in Eq. (4), is the opposite of the source correction, C_s to be effected when computing a mantle magnitude (Okal and Talandier, 1989).

In the case of a single force, we follow a similar strategy, and define the logarithmic average excitability, L_{av} as

$$L_{av} = \log_{10} \left[\frac{1}{N} \sum E^{\text{SF}} \right] \quad (5)$$

the average being taken over a large number of geometries. Since only two angles are involved for a single force source, we restrict the averaging to $N = 342$ geometries. Also, since single forces (generally interpreted as involving surface processes such as landslides), are expected to be shallow, we computed L_{av} for depths ranging from 4 to 20 km (in an average, i.e., oceanic model). Figure 1(a), directly comparable to Fig. 3 of Okal and Talandier (1989), presents the variation of L_{av} with period. A unit force of 10^{20} dynes is assumed, and therefore the units of K_i^{SF} are now 10^{-20} cm/dyn.

Following the approach in Okal and Talandier (1989), we then regress the shallowest of the curves on Fig. 1(a) as the cubic spline

$$L^{\text{SF}} = -C_s^{\text{SF}} = -1.3386\theta^3 + 0.71273\theta^2 + 0.62644\theta - 3.6122. \quad (6)$$

Again, this would be the opposite of the source correction to be used in a magnitude computation, hence the negative sign in (6). Figure 1(b) shows that the influence of depth on the error inherent in using (6) instead of the true excitation remains negligible at all periods greater than 35 s.

The relative efficiency $R_{\text{SF/DC}}$ of single forces and double couples for the excitation of Rayleigh waves can then be studied by comparing Eqs. (4) and (6); Fig. 2 plots the difference $L^{\text{SF}} - L^{\text{DC}}$, and shows that single forces are, relative to double-couples, increasingly efficient in their Rayleigh wave excitation, as the period T grows. A simple physical argument to explain this trend is as follows: single forces excite normal modes proportionally to the component of eigendisplacement along the force at the particular source depth, while double-couples excite proportionally to eigenstrain. One would then expect their relative efficiency to be proportional to the wavelength $\lambda = 2\pi a/l$. Appendix A details the derivation of the formula

$$R_{\text{SF/DC}}(T) = \frac{F_0}{M_0} \cdot 2.65 \frac{a}{l} = \frac{F_0}{M_0} \cdot \frac{2.65}{2\pi} cT, \quad (7)$$

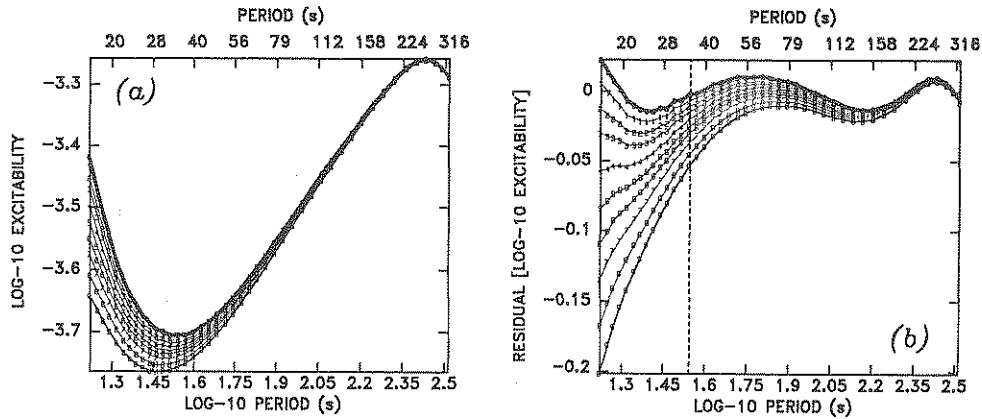


Fig. 1. (a) Logarithmic average excitability as defined by (5) in the case of a single force, plotted as a function of period and depth. The various symbols (from 0 to 9) refer to 10 sampling depths between 4 and 20 km. The thicker trace corresponds to 4 km, which is retained for the computation of L^{SF} (6). (b) Same as left, after the correction C_s^{SF} , given by (6) has been applied. Note that beyond 35 s (dashed line), the maximum error remains less than 0.05 units of magnitude. This figure is directly comparable to Fig. 3 of Okal and Talandier (1989) in the case of double-couples.

where c is phase velocity and T period, under the assumption of shallow sources in a homogeneous Poisson half-space. Figure 2 shows that the difference between Eqs. (4) and (6), derived from the real Earth model PREM (Dziewonski and Anderson, 1981), deviates a maximum of 0.08 unit of magnitude from this estimate.

2.2 Love waves

Similar calculations can be made for Love waves. We refer to Kanamori and Stewart (1976) and Okal and Talandier (1990) for the following expression of the excitation of a Love wave by a double-couple, which replaces Eq. (1)

$$M_0 \cdot E^{DC:L} = M_0 \left[\frac{1}{U} |iq_L L_1 l^{3/2} + p_L L_2 l^{5/2}| \right]. \tag{8}$$

In the case of a single force, Eq. (2) is replaced by

$$F_0 \cdot E^{SF:L} = F_0 \left[\frac{1}{U} |-iq_{FL} L_1^{SF} l^{3/2}| \right] \tag{9}$$

with the new coefficient L_1^{SF} related to its double-couple counterparts by:

$$L_1^{SF} = L_2 r_s. \tag{10}$$

Finally, the single force trigonometric coefficient is now $q_{FL} = -\sin \psi \sin \phi$.

The relative efficiency of single forces and double couples is given in Appendix A as

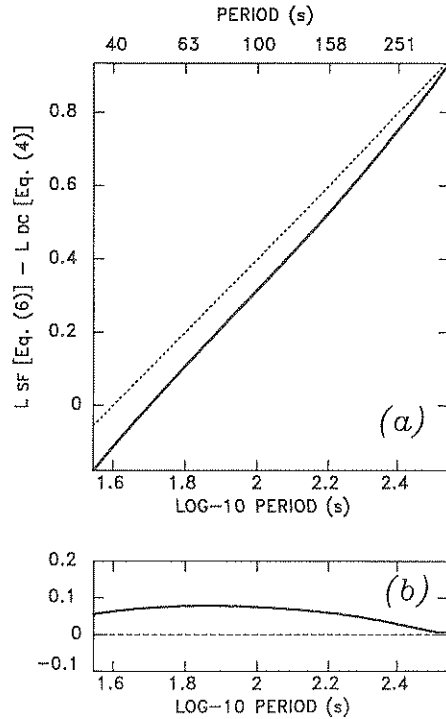


Fig. 2. (a) Plot of the difference in logarithmic average excitability between single forces and double-couples of identical source time functions. The thick trace represents the quantity $L^{SF} - L^{DC}$, as given by Eqs. (6) and (4). Note that it grows slightly faster than ω (the dotted line on the figure). (b) Residual between $L^{SF} - L^{DC}$, as plotted on (a), and $\log_{10} R_{SF/DC}$, as defined in (7), plotted in magnitude units. Note excellent agreement.

$$L_{SF/DC}(T) = \frac{F_0}{M_0} \cdot 1.25 \frac{a}{l} = \frac{F_0}{M_0} \cdot \frac{1.25}{2\pi} cT. \tag{11}$$

In conclusion, and for both types of surface waves, the relative efficiency of a single force (exciting proportionally to displacement) with respect to a double couple (exciting proportionally to strain) is proportional to wavelength, and thus grows with period slightly faster than T , since c in Eqs. (7) or (11) is itself a slowly growing function of T . It should be emphasized, however, that (7) and (11) are the result of averaging the excitation over many geometries of single forces and double-couples. A direct comparison of individual sources may not necessarily follow the same behavior with period, as will be more amply discussed in Sec. 4 and Appendix B.

2.3 Body waves

We refer for example to Aki and Richards (1980; pp. 74–81) for the classical expressions of the far-field amplitudes of the P wave generated by a point source single

force with time history $F_0(t)$:

$$u_i^{\text{SF}}(x, t) = \frac{1}{4\pi\rho V_p^2} \gamma_i \gamma_j \frac{1}{r} F_0(t - r/V_p) \quad (12)$$

and by a point source double-couple with time history $M_0(t)$:

$$u_i^{\text{DC}}(x, t) = \frac{1}{4\pi\rho V_p^3} A_i^{\text{FP}} \frac{1}{r} \dot{M}_0(t - r/V_p). \quad (13)$$

In these expressions, ρ and V_p are the density and P-wave velocity at the source, r is the distance to the station along the ray, and A_i^{FP} , γ_i , and γ_j are trigonometric coefficients (of order 1) describing the orientation of the source and of the receiver component u_i with respect to the ray. In the frequency domain, and for comparable source time functions (e.g., two Heaviside functions), the ratio of these displacements will be proportional to period; Appendix A details the derivation of their relative efficiency:

$$P_{\text{SF/DC}}(T) = \frac{F_0}{M_0} \cdot \frac{1.52}{2\pi} V_p T. \quad (14)$$

Similar results would be obtained for S waves.

3. Sources with Realistic Time Dependence

Of course, step function sources are unrealistic in nature. While they provide a good approximation for double couple sources, they are totally inadequate for single forces. We will describe here adequate source time functions, using the "Boxcar function"

$$\text{BOX}(t; t_0, t_1) = [H(t - t_0) - H(t - t_1)]. \quad (15)$$

3.1 Double-couples

In the case of double-couples, the source time function is usually modeled by introducing a rise time, τ_0 , such that the moment release rate takes the form

$$\dot{M}_0(t) = \frac{M_0}{\tau_0} \cdot \text{BOX}(t; 0, \tau_0). \quad (16a)$$

In the Fourier domain, this amounts to an additional factor

$$\frac{\dot{M}_0(\omega)}{M_0} = \left| \text{sinc} \frac{\omega\tau_0}{2} \right| \quad (16b)$$

for the spectral amplitudes. At high frequencies, the maximum spectral amplitude of a slow source decays like $1/\omega$, but at low frequencies the amplitude is unchanged. Figure 3 illustrates this well-known effect.

If the seismic release is slower in its build-up, the spectrum falls off faster at high frequencies, e.g., if

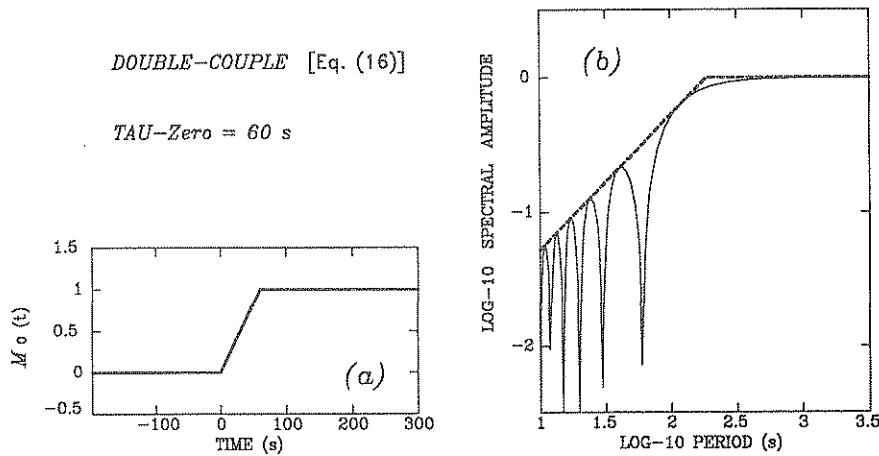


Fig. 3. Typical source time function for a double-couple source, modeled as Eq. (16). (a) Time-domain. (b) Fourier domain. The dashed line in (b) is the representation of the source spectrum as a corner function.

$$\dot{M}_0(t) = \frac{2M_0}{\tau_0} \cdot \text{BOX}(t; 0, \tau_0) \cdot \sin \frac{\pi t}{\tau_0}, \tag{17a}$$

then

$$\frac{\dot{M}_0(\omega)}{M_0} = \left| \frac{\omega_0^2}{\omega^2 - \omega_0^2} \cdot \cos \frac{\omega \tau_0}{2} \right|. \tag{17b}$$

3.2 Single forces

As discussed for example by Kawakatsu (1989), the condition that the whole Earth should not incur finite translation requires zero impulse, i.e., that the function $F_0(t)$ not only vanish as $t \rightarrow \infty$, but that its integral be zero. A simple representation of $F_0(t)$ can then be

$$F_0(t) = F_0 [\text{BOX}(t; 0, \tau_1) - \text{BOX}(t; \tau_1, 2\tau_1)]. \tag{18a}$$

With respect to a step function $F_0 H(t)$, this time function introduces an additional factor

$$\frac{\dot{F}_0(\omega)}{F_0} = 4 \sin^2 \frac{\omega \tau_1}{2} \tag{18b}$$

to the spectral amplitude of the excitation. Other, more realistic time functions could include a single complete period of a sinusoid

$$F(t) = F_0 \cdot \text{BOX}(t; 0, 2\tau_1) \cdot \sin \frac{\pi t}{\tau_1} \tag{19a}$$

whose contribution to the spectral amplitude is

$$\frac{\dot{F}_0(\omega)}{F_0} = \left| \frac{2\omega\omega_1}{\omega^2 - \omega_1^2} \cdot \sin \frac{\omega\tau_1}{2} \right| \tag{19b}$$

(with $\omega_1 = \pi/\tau_1$) or a function similar to (18a), but asymmetric, such as

$$F(t) = F_0 \left[\text{BOX}(t; 0, \tau_2) \cdot \sin \frac{\pi t}{\tau_2} - \frac{\tau_2}{\tau_3} \cdot \text{BOX}(t; \tau_2, (\tau_2 + \tau_3)) \cdot \sin \frac{\pi(t - \tau_2)}{\tau_3} \right]. \tag{20}$$

In particular, Eq. (19) approaches the models used by Kanamori *et al.* (1984) for the Mount St. Helens eruption ($\tau_1 = 120$ s), and Eq. (20) that for the 1929 Grand Banks earthquake ($\tau_2 = 15$ s; $\tau_3 = 35$ s) (Hasegawa and Kanamori, 1987).

These various sources all share the common property that, relative to a Heaviside function, their spectrum falls off like ω^2 at very low frequencies, a direct consequence of the zero impulse constraint. Figures 4–6 illustrate the behavior of the sources described in (18–20), both in time and frequency domains. On these figures, the dashed lines are the asymptotic behavior of the Fourier factors such as (10b) and (11b) for $\omega \rightarrow 0$, and in the case of $\omega \rightarrow \infty$, of the maxima of the spectral amplitude, without regard to the fast oscillations in the spectra.

3.3 Comparison of realistic sources

The subject of the next few sections is to discuss the possibility of identifying single forces as seismic sources, based on single-station records. Kawakatsu (1989) has demonstrated the feasibility of applying inversion theory to recover a centroid single force, and developed a method parallel to Dziewonski *et al.*'s (1981) centroid moment tensor inversion. He was further able to achieve significant improvements in variance reduction by using single forces to model the 1980 Mount St. Helens eruption, and the 1974 Mantaro landslide in Peru.

In this paper, we concentrate on single-station recordings, and address the

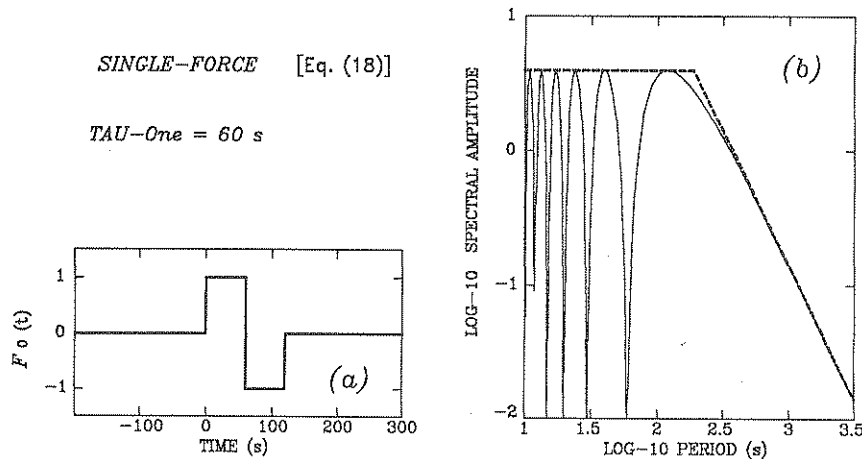


Fig. 4. Same as Fig. 3, for a single force, modeled as Eq. (18).

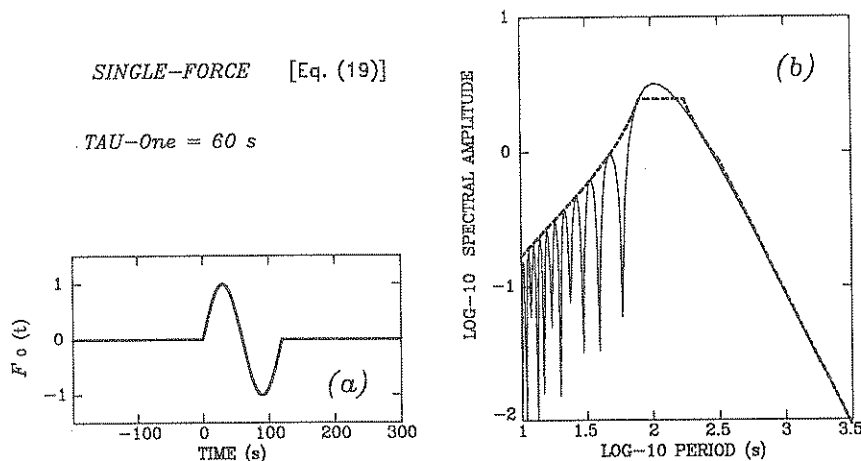


Fig. 5. Same as Fig. 3, for a single force, modeled as Eq. (19).

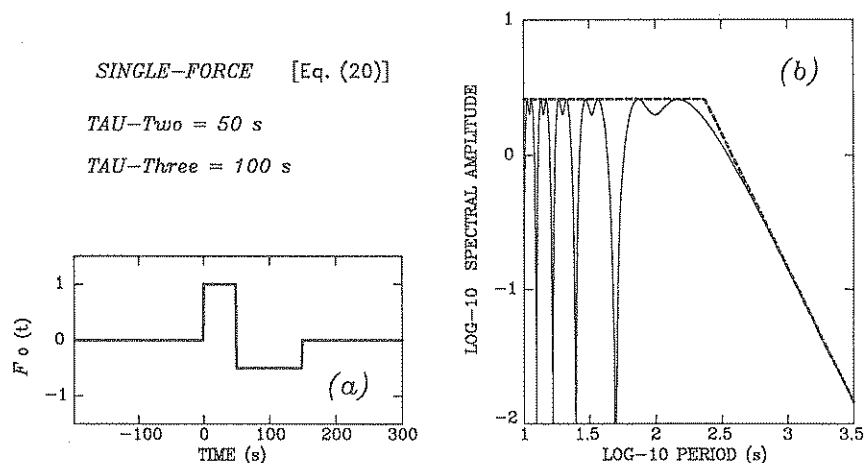


Fig. 6. Same as Fig. 3, for a single force, modeled as Eq. (20).

following question: Is it possible, in real time, and using only the records of a single station, to recognize the single force character of a teleseismic source? We are motivated in this approach by the context of tsunami warning on a remote island, a situation requiring real-time evaluation of the tsunamigenic potential of a large teleseismic source. We start by analyzing theoretically a number of parameters (shape of spectra, Love-to-Rayleigh ratios, etc.), and then discuss the results of a single-station inversion of theoretical spectra.

3.4 Shape of the spectra

We start by comparing the general shape of the Rayleigh wave amplitude spectra

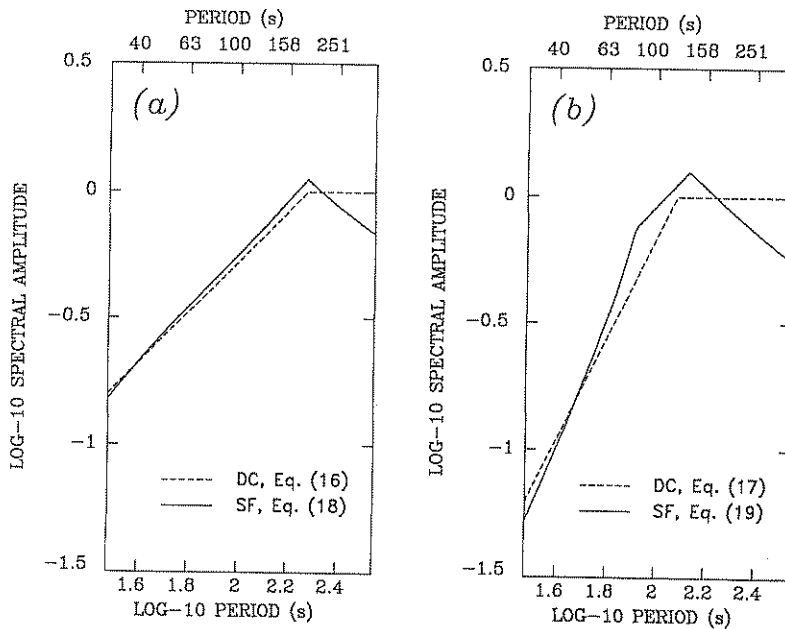


Fig. 7. Comparison of surface wave spectra for realistic single force and double-couple sources. The solid lines plot in logarithmic scale the combination of the relative efficiency of the single force, as given by (7), and of Fourier amplitude of the source time function. (a) Double-boxcar function (18). (b) Single-period sinusoid (19). In both cases, the dotted lines are the spectra of double-couples with source time functions matching the high-frequency part of the spectrum. See text for details.

of realistic single force and double-couple sources. For this purpose, we ignore the rapid oscillations in the spectra, and model them as “corner” functions, made of a combination of straight segments. For example, we can model the spectral amplitude of a slow double-couple (16b) with the familiar corner function: $[M_0(\omega)/M_0=1$ for $\omega \leq 2/\tau_0$; $M_0(\omega)/M_0=2/\omega\tau_0$ for $\omega \geq 2/\tau_0]$. Similarly, the spectral amplitude of the double-boxcar function (18b) can be modeled as $[\omega^2\tau_1^2$ for $\omega \leq 1/\tau_1$ and 1 for $\omega \geq 1/\tau_1]$. The corner functions are shown as the dashed lines on Figs. 3–6. We study the relative excitation characteristics of single forces and double couples through the quantity $[R_{SF/DC}(T) \cdot \hat{F}_0(\omega)/F_0]$, which is plotted as the solid traces on Fig. 7, using logarithmic coordinates. We purposely restrict the period range in this figure to 35–300 s, which is representative of typical records of surface waves. We use a source function given by Eq. (18) on Fig. 7(a), and by Eq. (19) on Fig. 7(b). In both cases, $\tau_1=60$ s.

In the high-frequency part of the spectrum, it is immediately apparent that the general behavior of the single forces is indistinguishable from that of an adequate double-couple. The single force’s advantage in excitation, given by (7), can be entirely compensated by a difference in source time function. For example, a double-boxcar single force (18) has a surface-wave high-frequency spectrum grossly equivalent to that

of a ramp double-couple (Eq. 16; dotted line on Fig. 7(a)); a full sinusoid single force (19) could be interpreted as a tapered, slowly growing double-couple (17; dotted line on Fig. 7(b)), given adequate choices of characteristic times τ_0 and scalar moments M_0 : this would only require that the moment rate release $\dot{M}(t)$ have the same high-frequency behavior as the force time function $F(t)$, in other words, that $M(t)$ be comparable to the primitive of $F(t)$.

The situation is of course different at the low-frequency end of the spectrum. The phase velocity c in (7) increases slowly with period, and so, the spectrum of the single force decays slightly slower than ω relative to that of the double-couple, through the combination of c/ω in (7) and ω^2 in (18b), (19b), etc. Thus, the single force has the inherent capability of producing a deficient spectrum at very low frequencies. Note that this point is mentioned (in general terms) by Kawakatsu (1989). However, from an operational point of view, it is difficult to successfully use this property in real-time to identify the single force character of a source. Most such events, associated with slumps or landslides are by nature slow, with characteristic times τ approaching 100 s. Figure 7 shows that the teleseismic amplitude spectrum does not become substantially deficient in the period range of readily observable mantle waves. Only for $T \geq \pi\tau_1$ (in practice beyond 300 s), would this deficiency be detectable. Similar results obviously hold in the case of Love waves, and we conclude that the general shape of the source spectrum of a teleseismic surface wave cannot be used to distinguish between the two kinds of source, except at the very lowest frequencies, which most often escape routine seismological observation.

3.5 Love to Rayleigh ratios

We further examine the question of the relative excitation of Love and Rayleigh waves by both double couples and single forces. The prominence of one type of waves at the expense of the other could be a significant discriminant, easy to utilize, even visually, in an observatory environment. For this purpose, it is possible to compare the average ratios $L_{SF/DC}$ and $R_{SF/DC}$ given by (11) and (7), and to form their quotient, which will also represent the quotient of a typical Love-to-Rayleigh spectral ratio for waves excited by a single force, to its counterpart for double-couples. At any given period T , this quotient is $2.12 c_L(T)/c_R(T)$, where the phase velocity c are indexed according to the nature of the wave. Phase velocities for Love and Rayleigh waves of similar periods are always very comparable; in the PREM model, between 40 and 2,500 s, c_L is on the average 1.07 times c_R . Consequently, and assuming an identical level of Rayleigh generation, a single force will generate Love waves on the average 2.3 times stronger than a double-couple. While this number is in itself interesting, and in agreement with Kanamori and Given's (1982 a) initial observation for the Mount St. Helens source, it must be remembered that it represents an average over many focal geometries. In this respect, it is very comparable to the fluctuations of relative Love-to-Rayleigh amplitudes due to focal and station-receiver geometry, and bears no promise for the systematic identification of single forces based on one-station recordings.

3.6 Use of body waves: $m_b : M_s$ or $m_b : M_0$ relations

We investigate in this section the possibility of a difference in the relative excitation

of body and surface waves by the two kinds of sources. Comparing Eqs. (7) and (14), we see that the relative excitation of body (P) and surface (Rayleigh) waves is controlled by the quantity

$$\frac{P_{SF/DC}}{R_{SF/DC}} \cdot \frac{\dot{F}_0(\omega_P)}{M_0(\omega_P)} \cdot \frac{\dot{M}_0(\omega_R)}{\dot{F}_0(\omega_R)} = 0.57 \cdot \frac{V_P}{c_R} \cdot \left[\frac{\omega_R}{\omega_P} \cdot \frac{\dot{F}_0(\omega_P)}{\dot{F}_0(\omega_R)} \cdot \frac{\dot{M}_0(\omega_R)}{M_0(\omega_P)} \right]. \quad (21)$$

In the case of P and Rayleigh waves, the two frequencies ω_P and ω_R can differ by as much as two orders of magnitude. However, if $M(t)$ behaves at high frequency like the primitive of $F(t)$ (which is necessary to model the surface wave spectra; see above discussion), then the combination in the brackets of (21) remains finite, and no anomaly exists between the relative sizes (or magnitudes) of surface and body waves. In other words, no $m_b : M_s$ or $m_b : M_0$ anomaly is expected beyond what could be expected from a "slow" double-couple.

4. Single Station Inversions

While the preceding sections have shown that a general comparison of spectral amplitudes is not a powerful discriminant between single forces and double couples, it has been suggested by Kawakatsu (1989) that a formal, one-station, inversion of multifrequency Love and Rayleigh spectra could discriminate between the two forms of sources. In principle, this could be due to two factors: the variation with frequency of the specific excitation coefficients related to individual geometries (as opposed to the average excitabilities as defined in the previous sections), and the inclusion of spectral phase information. In particular, an immediate consequence of Eq. (9) is that the source phase of a Love wave excited by a single force should always be $\pm \pi/2$ (For Rayleigh waves, it would depend on the inclination of the force with respect to the vertical, and equal $\pm \pi/2$ for a horizontal force). While a similar property would be expected for a double-couple with a pure vertical dip-slip mechanism, in practice it is not observed for shallow earthquakes, since the relevant excitation coefficients K_1 and L_1 vanish at the surface, and any small departure from the pure geometry is enough to strongly affect the source phase.

In order to explore this point more in detail, we carry out the following experiment: We synthesize Rayleigh and Love spectra at a single station for a number of double-couple and single force sources (including realistic time functions), and proceed to invert them, both into a single source, and into a double-couple. We then compare the performance of the inversions, as measured by the level of variance reduction. Table 1 lists the theoretical sources used in this experiment.

4.1 Double-couple sources

Sources C-1, C-2, and C-3 are the three fundamental double-couple configurations (SS, DS and T45 in Okal's (1988) notation); Source C-4 is rotated 45° in two directions. Station azimuths are given a variety of values, aimed at avoiding both nodes and lobes of the radiation pattern. Source depths are similarly taken in the range 10–20 km. Double-couple sources are given a "slow" time function of the form (16a), with $\tau_0 = 70$ s,

Table 1. Sources used in one-station inversion of synthetic spectra.

Single force sources							
Source	Amplitude (10^{20} dyn)	Colatitude ψ	Strike ϕ	Duration τ_1 (s)	Depth (km)	Station azimuth ($^\circ$)	
F-1	1	10	0	90	4	30	
F-2	1	45	0	90	4	60	
F-3	1	80	0	90	4	-35	
Double-couple sources							
Source	Amplitude (10^{27} dyn·cm)	Strike ϕ	Dip δ	Rake λ	Duration τ_0 (s)	Depth (km)	Station azimuth ($^\circ$)
C-1	1	0	90	0	70	15	30
C-2	1	0	90	90	70	10	-20
C-3	1	0	45	90	70	20	60
C-4	1	45	45	45	70	10	25

the corresponding factor in the frequency domain being

$$\frac{\dot{M}_0(\omega)}{M_0} = e^{-i\omega\tau_0/2} \operatorname{sinc} \frac{\omega\tau_0}{2}. \quad (22)$$

4.2 Single force sources

Sources F-1 and F-3 are nearly vertical and nearly horizontal single forces, respectively, the latter representative of the system proposed for Mount St. Helens (Kanamori *et al.*, 1984) or Kalapana (Eissler and Kanamori, 1987). Source F-2 is oriented 45° from the vertical. We place the source at 4 km depth in the PREM model, i.e., in the immediate vicinity of the seafloor of that oceanic model. Single force sources are given a time dependence of the form (18a), with $\tau_1 = 90$ s, representative of its value for the Mount St. Helens source (Kanamori *et al.*, 1982). With respect to a Heaviside force source, the additional factor in the frequency domain is:

$$\frac{\dot{F}_0(\omega)}{F_0} = -4 \sin^2 \frac{\omega\tau_1}{2} \cdot e^{-i\omega\tau_1}. \quad (23)$$

We consider a long-period spectrum, between 100 and 300 s, sampled at 25 frequencies. This is typical of the sampling allowed when using realistic windows of surface wave energy; higher-frequency signals could be significantly affected by lateral heterogeneity. When inverting for a single force source, we solve for the three components of the force, in the form of its amplitude F_0 , colatitude ψ , and strike ϕ . We loop over many values of source depth (between 3.5 and 10 km) and duration τ_1 , and study the variance reduction as a function of these parameters. When inverting for a double-couple,

we solve for the 5 independent components of a deviatoric moment tensor, and retain the most significant double-couple, which we describe through its moment M_0 , strike ϕ , dip δ , and rake λ , the conventions being those of Kanamori and Cipar (1974). The minor double couple component was usually found to be less than 15% of the major double couple. The source depth of the double couple is allowed to vary through the full range of shallow hypocenters (4 to 75 km).

4.3 Results

Results are listed in Tables 2 and 3. As expected, inversion for the proper kind of source yields nearly perfect results: both for forces or double-couples, the geometry of the source is recovered within a few degrees, and the source duration to an accuracy of 1 s. There can be a small amount of trade-off between source depth and scalar moment in the case of SS and T45 mechanisms.

In the case of cross-over inversions (e.g., inverting a double-couple spectrum into a single force), the quality of the inversion as measured by the variance reduction is consistently at the 70% level ($\pm 5\%$), a figure comparable to, if not better than, the typical quality of the moment tensor inversions routinely achieved in source mechanism studies (Dziewonski *et al.*, 1981; Kawakatsu, 1989). It is then doubtful that inversions of actual data could discriminate between the two kinds of sources. In several instances, the inversion can converge on several equally satisfactory solutions, differing mainly in source duration.

There are however two significant exceptions to this pattern. First, a vertical force (F-1) can be inverted to near perfection into a shallow T45 mechanism hinged in the direction of the observing station. This merely expresses the fact that both of these systems generate finite Rayleigh waves, but no Love waves (this possibility would disappear for a multiple station inversion).

Second, a shallow pure dip-slip mechanism on a vertical fault (C-2) cannot be inverted well into a single force, the variance reduction remaining under 50%. Such a mechanism generates both Rayleigh and Love waves vanishing as the source depth approaches the surfaces (or the bottom of the sea). However, their behavior with frequency is profoundly different. As detailed in Appendix B, it can be shown that while shallow pure strike-slip (SS) mechanisms generate Love and Rayleigh waves of comparable spectra amplitudes, the ratio $E^{DC}/E^{DC:L}$ of excitation of Rayleigh and Love waves behaves like $\omega^{3/2}$ in the DS geometry. For single forces, Eqs. (2), (3), (9), and (10) show that no such effects are expected, all excitation coefficients being proportional to K_2 and L_2 . In other words, it is impossible, with a single force, to create a strongly frequency-dependent deficiency of Rayleigh waves with respect to Love waves. This explains why the inversion of a C-2 spectrum for a single force source is unsuccessful. Moving the single force deeper would not help, since the coefficients K_2 and L_2 have vanishing depth derivatives at the surface.

However, the situation is different for the converse problem, i.e., inverting a horizontal force (F-2) spectrum into a double-couple. In order to fit the initial phase, the inversion seeks a DS mechanism, but at shallow depth, this is impossible due to the resulting strong deficiency in Rayleigh wave excitation. But the problem can be partially alleviated by sinking the source deeper, due to the finite value of the depth derivatives

Table 2. Results of inversion of single force synthetic spectra.

Inverted for a single force, $\Delta = 90^\circ$							
Source	Amplitude (10^{20} dyn)	Colatitude ψ	Azimuth ϕ	Duration τ_1 (s)	Depth (km)	Variance reduction	
F-1	1.02	10	1	90	6.5	99%	
F-2	1.01	45	1	90	6.0	99%	
F-3	1.00	80	0	90	4.0	100%	
Inverted for a single force, $\Delta = 89^\circ$							
Source	Amplitude (10^{20} dyn)	Colatitude ψ	Azimuth ϕ	Duration τ_1 (s)	Depth (km)	Variance reduction	
F-1	0.182	161	-165	37	7.0	99%	
F-1	0.696	159	-163	139	7.0	99%	
F-2	0.180	129	-168	35	7.0	98%	
F-2	0.695	130	-170	139	7.0	99%	
F-3	0.175	94	179	36	5.0	99%	
F-3	0.675	95	179	139	5.0	99%	
Inverted for a double-couple, $\Delta = 90^\circ$							
Source	Amplitude (10^{27} dyn·cm)	Strike ϕ	Dip δ	Rake λ	Duration τ_0 (s)	Depth (km)	Variance reduction
F-1	79.8	209	30	-91	81	3.5	94%
F-2	25.7	246	73	99	88	75	75%
F-3	2.88	195	79	4	17	75	75%
F-3	21.3	195	78	5	119	75	75%
Inverted for a double-couple, $\Delta = 89^\circ$							
Source	Amplitude (10^{27} dyn·cm)	Strike ϕ	Dip δ	Rake λ	Duration τ_0 (s)	Depth (km)	Variance reduction
F-1	23.4	215	30	97	32	3.5	95%
F-1	98.8	212	30	93	135	3.5	95%
F-2	18.7	259	76	298	142	75	75%
F-2	5.19	264	79	304	40	75	75%
F-3	6.82	195	85	3	70	75	75%

of K_1 and L_1 at shallow depths. This explains the significant increase in depth observed for this particular inversion (see Table 2). Finally, note that the combination of a vertical fault (C-2) and a pure shallow dip-slip mechanism (DS) represents a case when Eqs. (7) and (11) are violated. As noted earlier, these equations hold only for "average" orientations of both the force and the double-couple.

On the other hand, the similar increase in depth observed in the case of F-3 is related to the properties of the excitation coefficients K_2 and L_2 of the resulting SS

Table 3. Results of inversion of double couple synthetic spectra.

Inverted for a double-couple, $\Delta = 90^\circ$							
Source	Amplitude (10^{27} dyn·cm)	Strike ϕ	Dip δ	Rake λ	Duration τ_0 (s)	Depth (km)	Variance reduction
C-1	1.15	178	90	0	70	17	100%
C-2	1.10	360	90	90	70	10	100%
C-3	0.940	175	45	90	70	21	100%
C-4	0.931	47	46	41	70	11	100%
Inverted for a double-couple, $\Delta = 89^\circ$							
Source	Amplitude (10^{27} dyn·cm)	Strike ϕ	Dip δ	Rake λ	Duration τ_0 (s)	Depth (km)	Variance reduction
C-1	1.51	45	39	285	21	46	98%
C-1	8.82	45	39	284	124	46	98%
C-2	1.95	180	88	92	119	14	100%
C-3	0.841	22	85	344	21	34	98%
C-3	10.9	68	41	97	124	70	98%
C-4	0.949	55	72	148	19	35	98%
C-4	6.07	53	70	147	122	35	98%
Inverted for a single force, $\Delta = 90^\circ$							
Source	Amplitude (10^{20} dyn)	Colatitude ψ	Azimuth ϕ	Duration τ_1 (s)	Depth (km)	Variance reduction	
C-1	0.078	89	60	61	3.5	67%	
C-2	0.007	90	229	138	3.5	47%	
C-3	0.084	91	264	61	3.5	71%	
C-3	1.01	90	84	112	3.5	71%	
C-4	0.075	89	165	61	3.5	67%	
C-4	0.902	92	345	112	3.5	67%	
C-2 (limited to 4–5 mHz)	0.023	90	-119	35	3.5	88%	
Inverted for a single force, $\Delta = 89^\circ$							
Source	Amplitude (10^{20} dyn)	Colatitude ψ	Azimuth ϕ	Duration τ_1 (s)	Depth (km)	Variance reduction	
C-1	0.096	85	240	137	3.5	67%	
C-1	0.266	96	60	85	3.5	67%	
C-2	0.005	87	229	59	3.5	47%	
C-3	0.102	95	84	137	3.5	71%	
C-3	0.283	84	264	85	3.5	71%	
C-3	0.103	95	84	34	3.5	71%	
C-4	0.091	96	345	137	3.5	67%	
C-4	0.253	83	165	85	3.5	67%	
C-4	0.092	96	345	34	3.5	67%	

mechanism. These coefficients have vanishing derivatives at the surface. As a result, there is practically no depth resolution, and the choice of $h=75$ km is actually poorly constrained.

4.4 Influence of noise and systematic errors

As in all inversions of complex spectra, additional problems in real-life situations are the influence of noise and of errors in epicentral distance. We duplicated the experiments in Tables 2 and 3 in the presence of random noise, with a spectral amplitude reaching 10% of that of the signal. In addition, we also re-ran all the inversions with the distance artificially set at 89° (while the synthetics were computed for 90°), this level of imprecision being typical of a single-observatory location achieved in real-time. Results are given in Tables 4 and 5, and show that the variance reduction deteriorates

Table 4. Results of one-station inversion of single force synthetic spectra in the presence of 10% noise.

Inverted for a single force, $\Delta=90^\circ$							
Source	Amplitude (10^{20} dyn)	Colatitude ψ	Azimuth ϕ	Duration τ_1 (s)	Depth (km)	Variance reduction	
F-1	4.91	25	-140	97	7	94%	
F-2	1.16	44	-4	91	4	90%	
F-3	1.16	78	0	91	3.5	90%	
Inverted for a single force, $\Delta=89^\circ$							
Source	Amplitude (10^{20} dyn)	Colatitude ψ	Azimuth ϕ	Duration τ_1 (s)	Depth (km)	Variance reduction	
F-1	7.11	48	25	108	7	95%	
F-2	1.39	52	12	114	6	92%	
F-3	1.33	87	-1	114	3.5	92%	
Inverted for a double-couple, $\Delta=90^\circ$							
Source	Amplitude (10^{27} dyn·cm)	Strike ϕ	Dip δ	Rake λ	Duration τ_0 (s)	Depth (km)	Variance reduction
F-1	70.4	213	36	275	81	4	92%
F-2	25.7	246	73	99	88	75	75%
F-3	21.3	195	78	5	119	75	75%
Inverted for a double-couple, $\Delta=89^\circ$							
Source	Amplitude (10^{27} dyn·cm)	Strike ϕ	Dip δ	Rake λ	Duration τ_0 (s)	Depth (km)	Variance reduction
F-1	86.30	208	37	87	135	4	92%
F-2	18.5	265	79	306	143	75	75%
F-3	7.27	195	85	0	72	75	74%

Table 5. Results of one-station inversion of double-couple synthetic spectra in the presence of 10% noise.

Inverted for a double-couple, $\Delta = 90^\circ$							
Source	Amplitude (10^{27} dyn·cm)	Strike ϕ	Dip δ	Rake λ	Duration τ_0 (s)	Depth (km)	Variance reduction
C-1	6.54	22	38	73	80	75	91%
C-2	5.47	1	89	91	82	5	89%
C-3	6.15	260	53	294	78	75	90%
C-4	7.39	15	61	264	84	75	90%
Inverted for a double-couple, $\Delta = 89^\circ$							
Source	Amplitude (10^{27} dyn·cm)	Strike ϕ	Dip δ	Rake λ	Duration τ_0 (s)	Depth (km)	Variance reduction
C-1	9.22	54	44	298	122	45	95%
C-2	25.1	179	90	90	116	4	96%
C-3	6.96	201	85	16	123	42	95%
C-4	8.82	46	54	131	120	53	96%
Inverted for a single force, $\Delta = 90^\circ$							
Source	Amplitude (10^{20} dyn)	Colatitude ψ	Azimuth ϕ	Duration τ_1 (s)	Depth (km)	Variance reduction	
C-1	1.18	88	240	111	3.5	66%	
C-2	0.03	88	47	89	3.5	43%	
C-3	1.27	93	84	111	3.5	65%	
C-4	0.91	92	345	112	4	66%	
Inverted for a single force, $\Delta = 89^\circ$							
Source	Amplitude (10^{20} dyn)	Colatitude ψ	Azimuth ϕ	Duration τ_1 (s)	Depth (km)	Variance reduction	
C-1	0.38	89	59	88	3.5	61%	
C-2	0.11	93	49	110	3.5	47%	
C-3	0.45	93	264	89	3.5	62%	
C-4	0.35	89	165	88	3.5	61%	

significantly, although not alarmingly. However, the geometry and/or duration of the sources are not recovered; in particular distance trades off significantly with duration. This instability in the mechanism is partially alleviated in multistation inversions. Also, the presence of noise usually suppresses the occurrence of multiple solutions noted in some cross-over inversions.

4.5 A reflection on the case of the Kalapana earthquake

The Kalapana, Hawaii earthquake of 1975 has been described either as a nearly

horizontal single force (Eissler and Kanamori, 1987, 1988), or as a shallow, nearly pure DS double couple mechanism (Ando, 1979; Harvey and Wyss, 1986; Wyss and Kovach, 1988). Kawakatsu (1989) has shown that the variance reduction of a double-couple inversion is actually better than that of a single force (66% vs. 50%). Also, Glennon *et al.* (1989) have suggested a complex series of double-couple ruptures, lasting about 60 s. This controversy is in itself surprising, since the above discussion suggests that the particular geometry of the proposed double-couple should maximize the discriminating power of the inversions.

We note first that Glennon *et al.*'s (1989) study uses exclusively intermediate-period body waves (from 5 to 20 s). Kawakatsu's (1989) inversion is carried out in a relatively narrow band of frequency: from 4 to 5 mHz (200 to 250 s). As we have seen, the fundamental discriminant is the different behavior with frequency of Rayleigh and Love spectra. Narrowing the frequency window obviously reduces the power of the method. Indeed, we ran a single-force inversion of double-couple DS synthetic spectra limited to that particular frequency range, and were able to achieve a 88% variance reduction (see Table 2). On the other hand, Eissler and Kanamori's (1987) study favoring the single force mechanism is based (i) on IDA data (i.e., Rayleigh waves only) in the full spectral range 150–600 s; and (ii) on second passages of Love waves G_2 , from WWSSN and HGLP records, band-pass filtered around 100 s. Under these conditions, the double-couple Rayleigh deficiency at very-long periods could trade-off with the source time function of the single force source. The crucial discriminant in this situation would be the joint use of Rayleigh and Love waves over a broad range of frequencies, i.e., all the way to 300 s. Unfortunately, it is doubtful that such data exist, because of the absence or scarcity of adequate horizontal instruments at the time of the event. Note finally that the discriminant is not the absolute level of the Love-to-Rayleigh ratio at any given station (which varies like $\tan \phi$ or $\cot \phi$, and can be adjusted by rotating the orientation of either source), but rather its variation with frequency.

In conclusion of this section, single forces are expected to result in increasingly deficient surface wave spectral amplitudes at very long periods, for both Rayleigh and Love waves. This property starts to be identifiable at the very longest mantle wave periods (300 s and beyond). It is fundamental to include both types of waves in any such analysis, since the DS double-couple mechanism also generates a Rayleigh wave spectrum decreasing rapidly with increasing period. Therefore, and with particular reference to those events for which a controversy exists between a DS mechanism or a single force (Aleutian, 1946; Kalapana, 1975), the joint use of ultra-long period Love and Rayleigh waves would appear to be the most powerful discriminant.

5. Tsunami Excitation

In this section, we address the question of the relative efficiency of single forces and double couples for the excitation of tsunamis. Single forces have often been invoked to account for certain so-called "tsunami earthquakes," whose tsunamis were larger than predictable from the amplitude of their seismic waves. We will prove that a single force is actually a deficient tsunami generator.

Tsunami excitation can be studied readily in the framework of normal mode theory,

as introduced first by Ward (1980), and discussed later by Okal (1982, 1988). We will consider in this section a typical transpacific tsunami with a period of 1,000 s; in a typical ocean of average depth 4 km, the angular order of the corresponding normal mode is $l=200$. The calculation of the excitation of a tsunami wave by any system of forces proceeds exactly as in the case of a standard Rayleigh wave, with a few exceptions detailed in Appendix A. Equation (7) is now replaced by

$$T_{\text{SF/DC}}(T) = \frac{F_0}{M_0} \cdot 6.00 \frac{a}{l} = \frac{F_0}{M_0} \cdot \frac{6.00}{2\pi} cT. \quad (24)$$

Because the angular order of the tsunami ($l=200$) is about double that of a 100-s Rayleigh wave ($l=98$), their relative efficiencies, as defined by (7) and (24), are very comparable. However, the source time functions will play a fundamentally different role.

We want to test the hypothesis that a single force can explain a "tsunami earthquake." This would amount to saying that a single force excites tsunamis more efficiently than Rayleigh waves, the standard of comparison being an average double-couple. We quantify this hypothesis through the ratio Q between $T_{\text{SF/DC}}$ at a period T_T typical of a tsunami wave (say, 1,000 s) and $R_{\text{SF/DC}}$ at a period T_R typical of a mantle wave (say, 300 s), corrected for the spectral contribution of their respective source time functions. We assume a source of the form (18) for the single force, and (16) for the double-couple. Then

$$Q = \frac{6.00}{2.65} \frac{c_T T_T}{c_R T_R} \frac{\sin^2 [\omega_T \tau_1 / 2]}{\sin^2 [\omega_R \tau_1 / 2]} \frac{\text{sinc} [\omega_T \tau_0 / 2]}{\text{sinc} [\omega_R \tau_0 / 2]}. \quad (25)$$

If Q was significantly greater than 1, the amplitude of the single force required to account for mantle waves would result in a stronger tsunami than if modeled by a double-couple, and we could then conclude that single forces are, inherently, efficient tsunami generators. Unfortunately, it is easy to show that the ratio Q given by (25) always remains much smaller than 1: typical values of double-couple source times are at most $\tau_0 = 100$ s; only in the case of the 1960 Chilean earthquake, has an extremely slow dislocation been proposed, with τ_0 possibly on the order of 15 mn (Kanamori and Cipar, 1974; Kanamori and Anderson, 1975). In practice, at the period of tsunami waves, all known double-couple sources can be taken as Heaviside functions in the time domain. As for the typical range of times τ_1 proposed for single forces, they are usually tens of seconds (see Kawakatsu (1989) for a review). For τ_0 varying between 30 and 130 s, and τ_1 between 20 and 120 s, Q is found to range from 0.027 to 0.078.

In conclusion, all other parameters remaining comparable, *a single force is actually a deficient tsunami generator* and cannot explain a "tsunami earthquake." We surmise that the excessive tsunami amplitudes observed in connection with events successfully or tentatively modeled as single forces, are due to the penetration by the rupture of structures having deficient mechanical properties. We call these structures "sedimentary" but they could be of igneous fabric; all they need are rigidities μ significantly lower than that of consolidated crustal rocks. We refer to our previous study (Okal, 1988) for a discussion of the amplification of the tsunami excitation coefficient K_0 in such a layer. Since the physical interpretation of events modeled by a single force involves

surficial phenomena, such as landslides or slumps, such events are *by definition* perfectly shallow, and can be expected to result in strong motions of the sedimentary layers, generating a large tsunami, and as such, to be "tsunami earthquakes." But the latter property is not inherent in the nature of the source as a single force, as demonstrated convincingly by the capacity of regular double couples to model certain tsunami earthquakes, such as Peru (1960) or Tonga (1982) (Lundgren *et al.*, 1989; Pelayo and Wiens, 1990).

6. The Case of the CLVD (Tori-Shima Event of 1984)

In this section, we discuss briefly the extension of the previous results to the case of a Compensated Linear Vector Dipole [CLVD], as proposed by Barker and Kanamori (1986) and Kanamori *et al.* (1986), to model the Tori-shima underwater event of 13 June 1984.

A CLVD consists of a moment tensor with a vertical component $M_{zz} = M_0$, and perfect azimuthal isotropy in the horizontal plane: $M_{NN} = M_{EE} = -0.5M_0$. It can be regarded as the half-sum of two pure thrust fault (T45) mechanisms, rotated 90° apart. Equation (1) will remain valid with, in this case $s_R = 0.5$; $p_R = 0$; $q_R = 0$, regardless of the azimuth of the station. No Love waves are excited by a CLVD. As detailed in Appendix A, it is straightforward to show that the Rayleigh efficiency of the CLVD relative to an average double-couple is approximately 1.93, while for tsunamis, this number would be 1.44. The ratio of the two efficiencies (1.34) remains on the order of 1, and certainly cannot explain an order-of-magnitude disparity between the generation of tsunamis and mantle Rayleigh waves by a CLVD, as compared to a double-couple. However, an interesting fact is that the CLVD involves only the coefficient K_0 , which is precisely the one responsible for enhanced tsunami excitation in sediments (Okal, 1988). As such, a shallow CLVD penetrating softer layers as modeled in the case of Tori-shima by Kanamori *et al.* (1986), automatically becomes a tsunami earthquake.

7. Conclusions

The principal conclusions of the paper are:

1. The excitation of surface waves by single forces is proportional to displacement rather than eigenstrain, and thus would grow with period like c/ω , relative to an average double-couple, for identical source time functions. However, because of the condition of zero-impulse, any source time function for a single force brings an additional factor ω^2 with respect to the Heaviside function characteristic of a double-couple at long periods.

2. The resulting deficiency of energy at long periods, decaying like $\omega \cdot c$, i.e., slightly slower than ω , is difficult to detect in surface wave spectra, since it materializes only at the extreme low-frequency end of the mantle wave spectrum (300 s).

3. Individual single-station inversions of Love and Rayleigh spectra may in principle resolve a single force, but they must cover a broad enough range of frequencies. While the nature of the source can in principle still be retrieved, noise and systematic errors (e.g., on epicentral distance) can lead to significant instability in source geometry

and duration.

4. The joint use of *both Rayleigh and Love waves over a broad range of frequencies* is necessary to adequately resolve a horizontal single force from a pure vertical dip-slip double-couple, the fundamental discriminant being the *variation with frequency of the relative excitation of the two waves*. The controversy about the 1975 Kalapana earthquake could be explained by the use of band-pass filtered Love waves.

5. Because of the zero-impulse condition, and of the consequent ω^2 factor, single forces are strongly deficient tsunami generators, typically by 1.5 orders of magnitude with respect to double-couples. The observation that events potentially modeled as single forces are frequently found to generate anomalously strong tsunamis can be explained by their extreme shallowness, which casts the source (at least partially) into mechanically weak layers (e.g., sediments), thereby increasing tsunami excitation as explained in our previous paper (Okal, 1988).

6. Finally, in the case of Compensated Linear Vector Dipoles, such sources do not exhibit any substantial deficiency of excitation (except for the absence of Love waves, a reflection of their symmetry) for surface waves or tsunamis. Once again their ability to generate strong tsunamis is a direct consequence of their intruding sedimentary material.

This research was supported by the National Science Foundation, under Grant Number EAR-87-20549. I thank an anonymous reviewer for insightful scientific comments on a previous version of the paper.

REFERENCES

- Aki, K. and P. G. Richards, *Quantitative Seismology*, W. H. Freeman, San Francisco, 932 pp., 1980.
- Ando, M., The Hawaii, earthquake of November 29, 1975: low dip angle faulting due to forceful injection of magma, *J. Geophys. Res.*, **84**, 7616–7626, 1979.
- Barker, J. S. and H. Kanamori, Analysis of the teleseismic body waves for the June 13, 1984 earthquake near Tori-shima, Japan, *Eos. Trans. Am. Geophys. Union*, **67**, 1117, 1986 (abstract).
- Dziewonski, A. M. and D. L. Anderson, Preliminary reference earth model, *Phys. Earth Planet. Inter.*, **25**, 297–356, 1981.
- Dziewonski, A. M., T.-A. Chou, and J. H. Woodhouse, Determination of earthquake source parameters from waveform data for studies of global and regional seismicity, *J. Geophys. Res.*, **86**, 2825–2853, 1981.
- Eissler, H. K. and H. Kanamori, A single-force model for the 1975 Kalapana, Hawaii earthquake, *J. Geophys. Res.*, **92**, 4827–4836, 1987.
- Eissler, H. K. and H. Kanamori, Reply [to Wyss and Kovach], *J. Geophys. Res.*, **93**, 8083–8084, 1988.
- Glennon, M. A., W.-P. Chen, and J. L. Nábelek, Source Processes of three large Hawaiian earthquakes, *Eos. Trans. Am. Geophys. Union*, **70**, 397, 1989 (abstract).
- Harvey, D. and M. Wyss, Comparison of a complex rupture model with the precursor asperities of the 1975 Hawaii $M_s=7.2$ earthquake, *Pure Appl. Geophys.*, **124**, 957–973, 1986.
- Hasegawa, H. S. and H. Kanamori, Source mechanism of the magnitude 7.2 Grand Banks earthquake of November 1929: double-couple or submarine landslide?, *Bull. Seismol. Soc.*

- Am.*, **77**, 1984–2004, 1987.
- Kanamori, H., Mechanism of tsunami earthquakes, *Phys. Earth Planet. Inter.*, **6**, 346–359, 1972.
- Kanamori, H., Non-double-couple seismic source, Proc. XXIIIrd Gen. Assembl. Intl. Assoc. Seismol. Phys. Earth Inter, Tokyo, 1985, 425, 1985 (abstract).
- Kanamori, H. and D. L. Anderson, Amplitude of the Earth's free oscillations and long-period characteristics of the earthquake source, *J. Geophys. Res.*, **80**, 1075–1078, 1975.
- Kanamori, H. and J. J. Cipar, Focal process of the great Chilean earthquake, May 22, 1960, *Phys. Earth Planet. Inter.*, **9**, 128–136, 1974.
- Kanamori, H. and J. W. Given, Use of long-period surface waves for rapid determination of earthquake source parameters, *Phys. Earth Planet. Inter.*, **27**, 8–31, 1981.
- Kanamori, H. and J. W. Given, Analysis of long-period seismic waves excited by the May 18, 1980 eruption of Mount St. Helens—A terrestrial monopole?, *J. Geophys. Res.*, **87**, 5422–5432, 1982 a.
- Kanamori, H. and J. W. Given, Use of long-period surface waves for rapid determination of earthquake source parameters. 2. Preliminary determination of source mechanisms of large earthquakes ($M_s \geq 6.5$) in 1980, *Phys. Earth Planet. Inter.*, **30**, 260–268, 1982 b.
- Kanamori, H. and G. S. Stewart, Mode of strain release along the Gibbs Fracture Zone, Mid-Atlantic Ridge, *Phys. Earth Planet. Inter.*, **11**, 312–332, 1976.
- Kanamori, H., J. W. Given, and T. Lay, Analysis of seismic body waves excited by the Mount St. Helens eruption of May 18, 1980, *J. Geophys. Res.*, **89**, 1856–1866, 1984.
- Kanamori, H., G. Ekström, A. M. Dziewonski, and J. S. Barker, An anomalous seismic event near Tori-shima, Japan—A possible magma injection event, *Eos. Trans. Am. Geophys. Union*, **67**, 1117, 1986 (abstract).
- Kawakatsu, H., Centroid single force inversion of seismic waves generated by landslides, *J. Geophys. Res.*, **94**, 12363–12374, 1989.
- Lundgren, P. R., E. A. Okal, and D. A. Wiens, Rupture characteristics of the 1982 Tonga and 1986 Kermadec earthquakes, *J. Geophys. Res.*, **94**, 15521–15539, 1989.
- Okal, E. A., Mode-wave equivalence and other asymptotic problems in tsunami theory, *Phys. Earth Planet. Inter.*, **30**, 1–11, 1982.
- Okal, E. A., Seismic parameters controlling far-field tsunami amplitudes: a review, *Nat. Hazards*, **1**, 67–96, 1988.
- Okal, E. A., A theoretical discussion of time-domain magnitudes: the Prague formula for M_s and the mantle magnitude M_m , *J. Geophys. Res.*, **94**, 4194–4204, 1989.
- Okal, E. A. and J. Talandier, M_m : a variable period mantle magnitude, *J. Geophys. Res.*, **94**, 4169–4193, 1989.
- Okal, E. A. and J. Talandier, M_m : extension to Love waves of the concept of a variable-period mantle magnitude, *Pure Appl. Geophys.*, **134**, 355–384, 1990.
- Pelayo, A. M. and D. W. Wiens, The November 20, 1960 Peru tsunami earthquake: source mechanism of a slow event, *Geophys. Res. Lett.*, **17**, 661–664, 1990.
- Romanowicz, B. A. and P. Guillemant, An experiment in the retrieval of depth and source mechanism of large earthquakes using very long-period Rayleigh-wave data, *Bull. Seismol. Soc. Am.*, **74**, 417–437, 1984.
- Saito, M., Excitation of the free oscillations and surface waves by a point source in a vertically heterogeneous Earth, *J. Geophys. Res.*, **72**, 3689–3699, 1967.
- Ward, S. N., Relationship of tsunami generation and an earthquake source, *J. Phys. Earth*, **28**, 441–474, 1980.

Wyss, M. and R. L. Kovach, Comment on "A single-force model for the 1975 Kalapana, Hawaii earthquake" by Holly K. Eissler and Hiroo Kanamori, *J. Geophys. Res.*, **93**, 8078-8082, 1988.

APPENDIX A

We analyze the asymptotic behavior of the various excitation coefficients in the case of both seismic waves and tsunamis.

1. Rayleigh Waves

We start with the expression of the double-couple coefficients K_i , after Kanamori and Cipar (1974):

$$K_0 = A \left[\frac{2(3\lambda_s + 2\mu_s)}{\lambda_s + 2\mu_s} \cdot \left(y_1(r_s) - \frac{r_s}{3\lambda_s + 2\mu_s} y_2(r_s) - \frac{l(l+1)}{2} y_3(r_s) \right) \right] \quad (\text{A.1})$$

$$K_1 = A \frac{r_s}{\mu_s} \cdot y_4(r_s) \quad (\text{A.2})$$

$$K_2 = A \cdot y_3(r_s), \quad (\text{A.3})$$

where A is the constant

$$A = \frac{2l+1}{4\pi\omega^2 [I_1 + l(l+1)I_2] r_s} \quad (\text{A.4})$$

For large values of l , and sources close to the surface, the tractions y_2 and $l \cdot y_4$ go to zero, so that the prominent terms in (1) are the first and third terms of K_0 , and the last term involving K_2 . Furthermore, the aspect ratio of the displacement ellipse of the Rayleigh mode, $\varepsilon = l \cdot y_3(r_s)/y_1(r_s)$ is largely independent of frequency for shallow sources in the solid Earth, and approaches its value (-0.68) for a Poisson half-space. For the purpose of this calculation, we will take this as $-2/3$; we further assume a Poisson solid ($\lambda_s = \mu_s$). For large l , the first term in K_0 then becomes negligible with respect to the last one, and K_0 is found to behave like $[-(5/3)l^2 K_2]$. This result was also obtained by Okal (1988).

Similarly, according to Eqs. (3), K_0^{SF} would behave like $[-(3/2)l r_s K_2]$ and $K_1^{\text{SF}} = -r_s K_2$. As a result, the relative excitation of a Rayleigh wave by a single force F_0 and a double-couple M_0 is expected to be, in the large l approximation:

$$\frac{F_0}{M_0} \cdot \frac{r_s}{l} \cdot \frac{\left\langle \left| \frac{3}{2} s_F + i q_F \right| \right\rangle}{\left\langle \left| \frac{5}{3} s_R + p_R \right| \right\rangle} \quad (\text{A.5})$$

the brackets indicating an average over all possible geometries. The last part of this expression illustrates the fact that the trigonometric coefficients for single forces and

double couples have different such averages. Indeed, this ratio is found to be 2.65. Thus, the relative efficiency of a single force and a double couple for the excitation of a Rayleigh wave is, on the average,

$$R_{\text{SF/DC}}(T) = \frac{F_0}{M_0} \cdot 2.65 \frac{a}{l} = \frac{F_0}{M_0} \cdot \frac{2.65}{2\pi} cT \quad (\text{A.6})$$

where c is the phase velocity of the wave, and T the period.

2. Love Waves

An exactly similar approach shows that the relative efficiency of single forces and double couples at exciting Love waves is

$$L_{\text{SF/DC}}(T) = \frac{F_0}{M_0} \cdot \frac{r_s}{l} \cdot \frac{\langle |q_{\text{FL}}| \rangle}{\langle |p_{\text{L}}| \rangle}. \quad (\text{A.7})$$

The ratio of the average trigonometric coefficients is now 1.25, leading to

$$L_{\text{SF/DC}}(T) = \frac{F_0}{M_0} \cdot 1.25 \frac{a}{l} = \frac{F_0}{M_0} \cdot \frac{1.25}{2\pi} cT. \quad (\text{A.8})$$

3. Body Waves

We examine here the case of body waves, starting with Eqs. (12) and (13). If the amplitude of motion is measured along the direction of propagation of the P wave, $\gamma_i = 1$, $\gamma_j = \cos \alpha$, where α is the angle between the direction of the force F_0 and the ray, and $A^{\text{FP}} = \sin 2\theta \cos \phi$, where θ and ϕ are the colatitude and longitude of the direction of the ray in a system where the polar axis and the primary meridian are the slip vectors of the two fault plane solutions of the double-couple. As a result, the relative efficiency of P wave excitation by single forces and double couples with Heaviside source time functions is given by

$$P_{\text{SF/DC}}(T) = \frac{F_0}{M_0} \frac{V_p}{\omega} \frac{\langle |\cos \alpha| \rangle}{\langle |A^{\text{FP}}| \rangle}. \quad (\text{A.9})$$

The ratio of the average trigonometric coefficients is now 1.52, leading to

$$P_{\text{SF/DC}}(T) = \frac{F_0}{M_0} \frac{1.52}{2\pi} V_p T. \quad (\text{A.10})$$

The similarity between Eqs. (7) and (A.10) is not surprising, since a P wave can be considered as a superposition of Rayleigh overtones. For each branch p , the constant ($h = 2.65$ in (7)) would assume a different value ${}_p h$, because of different values of the ellipticity ϵ . The factor $1.52 V_p$ in (A.10) can be regarded as a weighted average of the terms ${}_p h_p c$ for the various overtone branches.

4. Tsunamis

The same formalism can be applied to the excitation of tsunamis. We refer to Ward (1980) for a discussion of the excitation of a tsunami, considered as a branch of normal modes of a gravitational Earth covered by an ocean, and to Okal (1982, 1988) for a discussion of its asymptotic properties. Equations (A.1)–(A.4) remain valid, but the properties of the “pseudo-Rayleigh” wave, i.e., the mostly elastic continuation of the tsunami wave into the solid Earth, differ from those a standard Rayleigh wave. While the shear traction $l \cdot y_4$ still vanishes at the sea-rock interface, the normal traction y_2 remains finite, and the ellipticity $l \cdot y_3 / y_1$ takes a different value. Both can be computed in the following way: Assume the solid Earth is a Poisson half-space. From standard Rayleigh theory, the vanishing of $l \cdot y_4$ at the top of the half-space results in an impedance

$$Z = \frac{y_2}{y_1} = -\mu k \frac{(2-\kappa^2)^2 - 4\sqrt{(1-\kappa^2)(1-\kappa^2/3)}}{\kappa^2 \sqrt{1-\kappa^2/3}} \quad (\text{A.11})$$

and an ellipticity

$$\varepsilon = \frac{ly_3}{y_1} = -\frac{(2-\kappa^2) - 2\sqrt{(1-\kappa^2)(1-\kappa^2/3)}}{\kappa^2 \sqrt{1-\kappa^2/3}}, \quad (\text{A.12})$$

where $k = c/\omega$ is the wave number and $\kappa = c/\beta$ the ratio of the phase velocity of the wave and of the shear velocity of the medium. For a standard Rayleigh wave, Z must vanish at the surface and Eq. (A.11) is used to infer the phase velocity ($\kappa = \sqrt{2-2/\sqrt{3}} = 0.9194$); Eq. (A.12) then yields $\varepsilon = -1/\sqrt{1+2\sqrt{3}} = -0.68$. In the case of a tsunami wave, c is controlled by the prominent gravity wave in the water column, and κ is very small (typically on the order of 0.05). In the limit $\kappa \rightarrow 0$, $Z \rightarrow (4/3)\mu k$ and $\varepsilon \rightarrow -1/3$.

As a result, both the second and third terms in K_0 (see Eq. (A.1)) remain important, and $K_0/l^2 K_2 \rightarrow 1$. Also, K_0^{SF} now behaves like $[3lr_s K_2]$. Equation (A.5) is then replaced by

$$\frac{F_0}{M_0} \cdot \frac{r_s \cdot \langle |3s_F + iq_F| \rangle}{l \langle |s_R + p_R| \rangle} \quad (\text{A.13})$$

The ratio of the averages of the trigonometric coefficients takes the substantially higher value 6.00, and thus (A.6) is replaced by:

$$T_{\text{SF/DC}}(T) = \frac{F_0}{M_0} \cdot 6.00 \frac{a}{l} = \frac{F_0}{M_0} \cdot \frac{6.00}{2\pi} cT. \quad (\text{A.14})$$

5. The Case of the CLVD

In the case of a Compensated Linear Vector Dipole, and since the trigonometric coefficients are always $s_R = 0.5$; $p_R = q_R = 0$, the excitation of any Rayleigh (or tsunami) mode is always $[0.5K_0 l^{-1/2}/U]$.

For a Rayleigh wave, $K_0/l^2K_2 \rightarrow -5/3$, and Eq. (A.5) is replaced by

$$R_{\text{CLVD/DC}} = \frac{5/6}{\left\langle \left| \frac{5}{3} s_R + p_R \right| \right\rangle} \quad (\text{A.15})$$

or about 1.93. Because this number is independent of frequency, no $M_s : M_0$ anomaly should be expected from a CLVD source. Indeed, the moment proposed by Kanamori *et al.* (1986) (4×10^{24} dyn·cm) and the reported $M_s = 5.5$ are in good agreement with the theoretical relation between moment and magnitude $M_s = \log_{10} M_0 - 19.46$, obtained by Okal (1989) for double-couples.

For a tsunami, $K_0/l^2K_2 \rightarrow 1$, and (A.13) is replaced by

$$T_{\text{CLVD/DC}} = \frac{1/2}{\langle |s_R + p_R| \rangle} \quad (\text{A.16})$$

or about 1.44.

APPENDIX B

The purpose of this section is to find asymptotic values for the relative excitabilities of Rayleigh and Love mantle waves by double-couples, in the limit of a very shallow source. We want to justify the observation that, as the period T increases in the range 100–300 s, pure dip-slip sources exhibit an increasingly strong deficiency in Rayleigh excitation, relative to Love waves. This property is apparent, for example in the excitation coefficients listed in Table A1 of Kanamori and Given (1981).

We start with Eqs. (1), (A.1) to (A.4), and their Love counterpart (8), where:

$$L_1 = B \frac{r_s}{\mu_s} y_2^T(r_s) \quad (\text{B.1})$$

$$L_2 = B y_1^T(r_s) \quad (\text{B.2})$$

with

$$B = \frac{2l+1}{4\pi\omega^2 l(l+1) I_1^T r_s} \quad (\text{B.3})$$

the superscript T identifying torsional modes, and the notation being that of Saito (1967).

Since y_4 and y_2^T vanish at the surface (which can be taken as the ocean bottom for a model such as PREM), their values at an asymptotically small depth h can be taken as $-h \cdot [dy_4/dr]_0$ and $-h \cdot [dy_2^T/dr]_0$ respectively, the subscript 0 referring to the surface. We use Saito's (1967) Eqs. (7) and (14) to obtain an estimate of these derivatives. For the Rayleigh case, assuming a Poisson solid ($\lambda_s = \mu_s$), and neglecting gravitational terms

$$\frac{dy_4}{dr} = -\frac{10\mu}{3} \frac{y_1}{r^2} - \frac{y_2}{3r} + \left[(4l(l+1) - 3) \frac{2\mu}{3r^2} - \omega^2 \rho \right] y_3 - 3 \frac{y_4}{r}. \quad (\text{B.4})$$

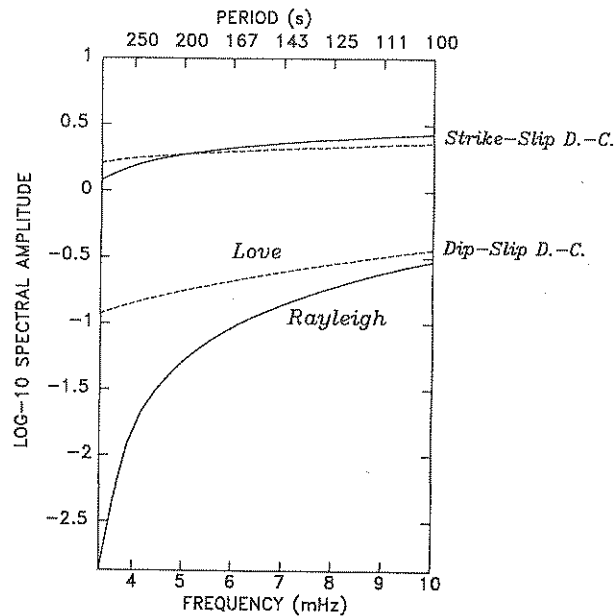


Fig. B1. Spectral amplitudes of shallow double-couples for Rayleigh (solid lines) and Love mantle waves (dashed lines) as a function of frequency. The geometries considered are pure strike-slip and pure dip-slip on a perfectly vertical fault, with the station located at an azimuth equally favorable to Love and Rayleigh waves ($\phi=45^\circ$ for DS and $\phi=22.5^\circ$ for SS). This figure illustrates the increasingly deficient excitation of Rayleigh waves relative to Love waves at longer periods, for the dip-slip mechanism.

At the bottom of the ocean, the last term vanishes, and y_2 takes the approximate value $[-\omega^2 \rho_{\text{water}} y_1 H]$ where H is the depth of the oceanic column. The ratio of the second to first terms in (B.4) is therefore

$$\frac{H}{10a} \cdot \frac{\rho_{\text{water}}}{\rho_s} l^2 \frac{c^2}{\beta_s^2}. \quad (\text{B.5})$$

At periods greater than 100 s, this ratio is at most of order 1. The third term in (B.4) is of order $(l^2 \mu/a^2)[8/3 - c^2/\beta_s^2]y_3$. In the large l limit, and close to the surface, the ellipticity ly_3/y_1 of a Rayleigh wave approaches -0.68 , the third term in (B.4) is of order l with respect to the first and second ones, and hence dominant. Because of the dispersion of c with frequency, its behavior is not simple, but it is found empirically that the non-dimensional bracket $[8/3 - c^2/\beta_s^2]$ varies approximately like ω between 100 and 300 s. $y_4(r_s)$ can then be written as $-h(\omega/\Omega_R)(l^2 \mu_s/a^2)y_3(r_s)$, where Ω_R is an adequate constant having dimensions of frequency. If, according to Kanamori and Cipar's (1974) conventions, y_1 is normalized to 1 at the surface, then $y_3 = -0.68/l$, and coefficients for DS and SS mechanisms then take the form $K_1 = n_1(\omega/\Omega_R)Al(h/a)$; $K_2 = n_2(A/l)$, where the n_i 's are non-dimensional constants of order 1.

Similarly, in the case of Love waves,

$$\frac{dy_2^T}{dr} = \left[(l(l+1) - 2) \frac{\mu}{r^2} - \omega^2 \rho \right] y_1^T - \frac{3}{r} y_2^T. \quad (\text{B.6})$$

Near the surface, the second term vanishes, but this time the non-dimensional bracket $[1 - c^2/\beta_s^2]$ in (B.6), always negative, decreases in amplitude with frequency, in practice like $\omega^{-1/2}$. If y_1^T is normalized to 1, the derivative becomes of order $(\omega/\Omega_L)^{-1/2} \mu l^2/a^2$, and we obtain $L_1 = n_3(\omega/\Omega_L)^{-1/2} B l^2 h/a$; $L_2 = B$.

In order to compare the excitations of Love and Rayleigh waves, we note that their phase velocities c are generally very comparable for mantle waves, i.e., that for a given period in the range studied (100 to 300 s), l takes similar values for both types of waves. We also find that, under the chosen normalization, the integrals I_1^T and $[I_1 + l(l+1)I_2]$ in (B.3) and (A.4) have comparable values (within a factor of 2) at similar frequencies; this being due to the largely comparable decay of the eigenfunctions with depth. Therefore B/A behaves like l^{-2} and we obtain the following two results:

- For strike-slip earthquakes, the relative excitation of Love and Rayleigh waves by shallow sources, controlled by the ratio $[lL_2/K_2]$, is of order 1;

- For dip-slip earthquakes, the ratio is now $[lL_1/K_1]$, which behaves like $\omega^{-3/2}$.

In other words for a pure dip-slip source, both Love and Rayleigh excitation go to 0 as the source approaches the surface, but this deficiency in excitation becomes increasingly important for Rayleigh waves at longer periods. Figure B1 illustrates these results, which are also contained in the excitation tables listed by Kanamori and Given (1981).